ISSN 1070-3284, Russian Journal of Coordination Chemistry, 2024, Vol. 50, No. 2, pp. 156–162. © Pleiades Publishing, Ltd., 2024.

Rhenium(V) Tris(pyrazolyl)borate Thiolate Complex with the Disulfide Bridging Ligand: Synthesis and Structure

I. V. Skabitskii[a], * and S. S. Shapovalov[a]

[a] *Kurnakov Institute of General and Inorganic Chemistry, Russian Academy of Sciences, Moscow, Russia*

**e-mail: skabitskiy@gmail.com*

Received May 12, 2023; revised June 5, 2023; accepted June 27, 2023

Abstract—The reaction of TpReOCl(S^{t}Bu) (Tp = tris(pyrazolyl)borate anion) with sodium disulfide in dimethoxyethane affords the new binuclear rhenium complex $[TpReO(\mu\text{-}S^tBu)]_2(\mu\text{-}S_2)$ (**I**). Complex **I** can also be synthesized by the reaction of $TpReO(S^tBu)_2$ with a suspension of manganese(II) bromide in toluene accompanied by the dealkylation of one of the ligands to form one more new complex $[TpReO]_2(\mu\text{-}S_2)(\mu\text{-}S)$ (**II**) containing the bridging sulfide and disulfide ligands. The structures of two crystalline solvates of complex **I** with dichloromethane containing the molecules with different conformations of the Re_2S_2 fragment (**Ia** and **Ib**) and complex **II** are studied by X-ray diffraction (XRD) (CIF files CCDC nos. 2262677, 2262678, and 2267423 for **Ia**, **Ib**, and **II**, respectively).

Keywords: rhenium complexes, thiolate complexes, disulfide ligand, tris(pyrazolyl)borate

DOI: 10.1134/S1070328423601152

INTRODUCTION

Tris(pyrazolyl)borate anions are tridentate ligands and form stable complexes with transition metals. They found wide use in coordination chemistry [1]. The rhenium complexes with tris(pyrazolyl)borate and thiolate ligands were studied in detail as models for the catalytic desulfonation [2]. Of the complexes with sulfide ligands, only Tp^*ReSCl_2 was synthesized but was not structurally characterized [3]. Rhenium tris(pyrazolyl)borate complexes with the disulfide ligand were not described, and the number of these complexes with other metals are not high.

The molybdenum tris(pyrazolyl)borate sulfur-containing complexes $Tp^{iPr}MoO(OAr)S$ were synthesized by the addition of triethylphosphine to one of the oxygen atoms in the $Tp^{iPr}MoO_2(OAr)$ dioxo complex followed by the substitution of $OPEt_3$ by the sulfur atom under the action of methylthiirane [4]. According to the X-ray absorption spectroscopy (XAS) data, these complexes are monomeric in solutions and can exist in the crystalline phase in both the monomeric form (Ar = C_6H_4-^{s}Bu-2, C_6H_4-^{t}Bu-2, C_6H_4Ph-4) and as dimers with the disulfide bridging ligand (Ar = C_6H_4-^{t}Bu-3, $C_6H_3{}^t Bu_2$-3,5, C_6H_4Ph-3, Ph) depending on the aryloxide substituent. The hydrolysis of this type complexes leads to the substitution of two alkoxide groups by the bridging oxo ligand with the retention of the disulfide fragment.

The reaction of $(Ph_3Sn)_2S$ with $TpMoCl_2(NO)$ afforded the nitrosyl complex $[TpMoCl(NO)]_2(\mu\text{-}S_2)$ in a low yield [5].

The neutral dimeric tungsten complex $[Tp^*WS_2]_2(\mu\text{-}S_2)$ was synthesized by the oxidation of the Tp^*WS_3 anion with silver thiocyanate [6] and used as the initial compound for the preparation of a series of heterometallic sulfide halide clusters with copper and silver having nonlinear optical properties.

The reaction of $[Tp_2Ru_2(\mu\text{-}Cl)(NO)_2(MeCN)]$ with elemental sulfur affords the tetranuclear ruthenium complex $[(Tp_2Ru_2(\mu\text{-}C_3H_3N_2)(\mu\text{-}Cl)(NO))_2(\mu\text{-}S_2)][BF_4]_2$ in which the bridging disulfide ligand links two dimeric fragments along with the three-bridging dimer $Tp_2Ru_2(\mu\text{-}Cl)(\mu\text{-}NO)_2(\mu\text{-}S_2)$ [7].

The purpose of the work is the synthesis of the disulfide complex $[TpReO(\mu\text{-}S^tBu)]_2(\mu\text{-}S_2)$ (**I**), which is the single soluble product in the reaction of $TpReO(S^tBu)_2$ with $Mn(CO)_5Br$. It seemed important to find other methods for its synthesis for the preparation of a series of the related heterometallic sulfide clusters.

EXPERIMENTAL

All procedures during the synthesis and product isolation were carried out in anhydrous solvents under a pure argon atmosphere. IR spectra were recorded on a Bruker Alpha spectrometer with a Bruker ATR Diamond accessory. ^{1}H NMR spectra were detected on a

Bruker AV 300 instrument. The ^{1}H chemical shifts are presented relative to tetramethylsilane. The syntheses of TpReO(S^{t}Bu)$_2$ and TpReOCl(S^{t}Bu) were carried out according to a published procedure [8].

Synthesis of [TpReO(μ-S^{t}Bu)]$_2$(μ-S$_2$) (I). *Method 1.* Sulfur (29 mg, 0.91 mmol) and naphthalene (20 mg, 0.16 mmol) were added to a sodium powder (21 mg, 0.91 mmol) in dimethoxyethane (5 mL). The powder was prepared by shaking molten sodium in xylene. The resulting suspension was magnetically stirred at 60°C for 24 h, then TpReOClS^{t}Bu (100 mg, 0.18 mmol, fivefold deficiency) was added, and the reaction mixture was stirred at 40°C for 12 h. The solvent was removed in vacuo, and the red-brown residue was extracted with toluene (10 mL). The extract was deposited on a column packed with silica gel (5 × 1 cm) in toluene. Unreacted green TpReOClS^{t}Bu and yellow-brown TpReO(S^{t}Bu)$_2$ were eluted with toluene (40 mL), and red compound **I** was eluted with a toluene–ethyl acetate (10 : 1) mixture (20 mL). The eluate was evaporated in vacuo, the residue was dissolved in CH_2Cl_2 (1 mL), and hexane (5 mL) was added. The red-brown crystals precipitated on holding at –25°C were decanted, washed with pentane (5 mL), and dried in vacuo. The yield was 16 mg (16%).

Method 2. Dibromine (50 μL, deficiency) was added to a manganese powder (100 mg) in acetonitrile (10 mL). The reaction mixture was stirred at 60°C for 1 h, a hot light brown solution was filtered and evaporated to dryness in vacuo, and the residue was dried at 150°C in vacuo. Toluene (5 mL) and TpReO(S^{t}Bu)$_2$ (107 mg, 0.18 mmol, deficiency) were added to the prepared beige-colored powder, and the resulting suspension was stirred at 80°C for 48 h. Then the dark red solution was filtered from the dark brown precipitate. Complex **I** was separated by chromatography from the unreacted initial compound and crystallized similarly to method 1. The yield was 24 mg (25%).

IR (ν, cm^{-1}): 3145 vw, 3123 br, vw 2955 br, vw 2912 vw, 2889 vw, 2854 vw, 2499 br, vw 1501 w, 1405 m, 1391 vw, 1360 vw, 1309 s, 1216 m, 1187 vw, 1158 vw, 1119 s, 1074 w, 1047 vs, 985 m, 934 vs, 917 vw, 889 vw, 856 vw, 818 vw, 793 w, 765 s, 756 vw, 712 vs, 661 w, 615 m, 576 vw, 551 vw, 532 vw, 485 vw, 462 vw, 436 vw, 418 vw.

^{1}H NMR (toluene-d^8; 298 K; δ, ppm): 1.80 (s, 9H, SC(CH_3)$_3$), 5.53 (t, $^3J_{H-H}$ = 2.1 Hz, 1H), 5.81 (t, $^3J_{H-H}$ = 2.4 Hz, 1H), 5.99 (t, $^3J_{H-H}$ = 2.4 Hz, 1H), 6.93 (dd, $^3J_{H-H}$ = 2.6 Hz, $^4J_{H-H}$ ~ 0.7 Hz, 1H), 7.23 (dd, $^3J_{H-H}$ = 2.4 Hz, $^4J_{H-H}$ ~ 0.8 Hz, 1H), 7.31 (dd, $^3J_{H-H}$ = 2.4 Hz, $^4J_{H-H}$ ~ 0.8 Hz, 1H), 7.57 (d, $^3J_{H-H}$ = 1.7 Hz, 1H), 8.50 (d, $^3J_{H-H}$ = 2.0 Hz, 1H), 8.54 (d, $^3J_{H-H}$ = 2.2 Hz, $^4J_{H-H}$ ~ 0.5 Hz, 1H).

For $C_{26}H_{38}B_2N_{12}O_2S_4Re_2$ (*FW* = 1073)

Anal. calcd., %	C, 29.10	H, 3.57	N, 15.67
Found, %	C, 28.68	H, 3.47	N, 15.02

Synthesis of [TpReO]$_2$(μ-S$_2$)(μ-S) (II). When synthesizing compound **I** for 72 h using method 2, a powder of complex **II** almost immediately precipitated upon the recrystallization of the eluate containing complex **I**. The yield of complex **II** was <1 mg.

IR (ν, cm^{-1}): 3116 br w, 3035 vw, 2514 br w, 1499 s, 1404 vs, 1387 w, 1308 vs, 1262 w, 1206 vs, 1186 vw, 1117 s, 1073 w, 1044 vs, 984 m, 931 br vs, 857 vw, 815 w, 788 w, 775 w, 757 m, 726 w, 709 br vs, 667 vw, 651 w, 616 m, 570 vw, 531 vw, 511 vw, 493 vw, 470 vw, 437 vw.

The crystals of complexes **I** and **II** suitable for XRD were prepared by the diffusion of pentane vapors into a solution of compound **I** in CH_2Cl_2.

XRD of complexes **I** and **II** was carried out on a Bruker Venture D8 diffractometer. An absorption correction was applied by multiple measurements of equivalent reflections using the SADABS program [9] for compound **Ia** and the TWINABS program [10] for compounds **Ib** and **II**. The structures were solved by a direct method and refined by least squares for F^2 in the anisotropic approximation of non-hydrogen atoms using the SHELX-2014 [11] and OLEX2 [12] software. The positions of hydrogen atoms were calculated geometrically. The crystallographic data and structure refinement parameters are given in Table 1. Selected bond lengths and bond angles in compound **I** are listed in Table 2.

The coordinates of atoms and other structural parameters were deposited with the Cambridge Crystallographic Data Centre (CIF files CCDC nos. 2262677, 2262678, and 2267423 for **Ia**, **Ib**, and **II**, respectively; http://www.ccdc.cam.ac.uk/data_request/cif).

Quantum-chemical calculations were performed in the framework of the density functional theory using the ORCA 5.03 software [13]. Geometry optimization of the complexes was performed using the PBE functional [14, 15] in the all-electron split valence double def2-SVP basis set [16] with the empirical D3BJ dispersion corrections [17, 18]. The activation energy was calculated using the PBE0 hybrid functional [19] in the split valence triple def2-TZVP basis set [16]. The electron density was calculated by the ZORA method taking into account scalar relativistic corrections [20, 21] in the all-electron split valence triple basis set adapted for this method [22, 23].

Table 1. Crystallographic data and structure refinement parameters for complexes **I** and **II**

Parameter	**Ia**	**Ib**	**II**
Empirical formula	$C_{26}H_{38}B_2N_{12}O_2S_4Re_2$	$C_{13.62}H_{20.24}BN_6OS_2Cl_{0.52}Re$	$C_{19}H_{22}B_2N_{12}O_2S_3Cl_2Re_2$
FW	1072.94	563.73	1011.58
Radiation (λ , Å)		MoK_α (λ = 0.71073)	
Temperature, K	100	100	100
Crystal system	Monoclinic	Triclinic	Monoclinic
Space group	*C*2/*c*	$P\bar{1}$	$P2_1/c$
a, Å	20.4820(16)	15.0275(6)	16.3187(6)
b, Å	11.0909(8)	18.8478(7)	12.9928(5)
c, Å	21.0234(15)	23.1384(9)	15.8950(6)
α, deg	90	103.2280(10)	90
β, deg	116.509(2)	93.7360(10)	116.2740(10)
γ, deg	90	109.9580(10)	90
V, Å^3	4273.7(6)	5922.6(4)	3022.0(2)
Z	4	6	4
ρ_{calc}, g/cm^{-3}	1.668	1.897	2.223
μ, mm^{-1}	5.893	6.452	8.431
F(000)	2072.0	3274.0	1912.0
Scan range, deg	4.292–65.49	3.622–61.114	4.242–55.812
Scan mode		ω	
Independent reflections (N_1)	7871 (R_{int} = 0.0544)	36882 (R_{int} = 0.05323)	7187 (R_{int} = 0.0574)
Reflections with $I > 2\sigma(I)$ (N_2)	7354	33022	6719
Number of refined parameters	220	1393	408
GOOF	1.076	1.088	1.067
R_1 for N_2	0.0200	0.0341	0.0279
wR_2 for N_1	0.0442	0.0751	0.0664
$\Delta\rho_{max}/\Delta\rho_{min}$, e Å^{-3}	1.42/–1.41	1.78/–1.38	1.23/–1.76

RESULTS AND DISCUSSION

The reaction of $TpReO(S^tBu)_2$ with an excess suspension of manganese bromide in toluene at 80°C affords the new complex $[TpReO(\mu\text{-}S^tBu)]_2(\mu\text{-}S_2)$ (**I**), which can be separated by chromatography from the unreacted initial compound. Attempts to increase the reaction time or $MnBr_2$ excess resulted in the formation of a number of unidentified by-products that impeded the isolation of the complex, among which one of the products of the further dealkylation and desulfonation was characterized by the XRD data as $[TpReO]_2(\mu\text{-}S_2)(\mu\text{-}S)$ (**II**) containing the sulfide and disulfide bridging ligands. A similar reaction with anhydrous $MnCl_2$ gives only insignificant quantities of $TpReOCl(S^tBu)$ [8] identified by TLC in comparison with the standard.

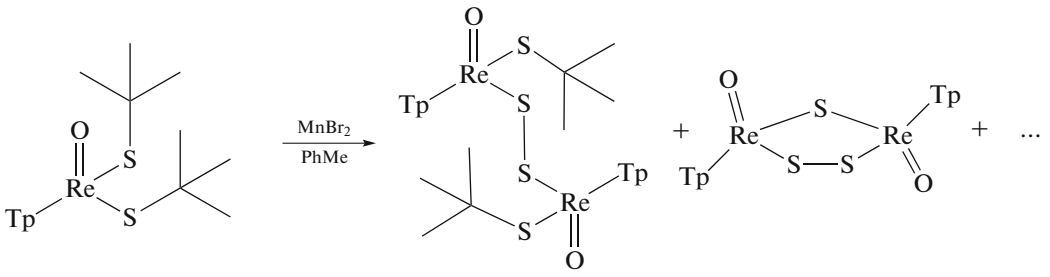

Table 2. Bond lengths and bond angles in the structures of complexes **Ia** and **Ib**

Bond	**Ia**	**Ib** molecule 1	**Ib** molecule 2	**Ib** molecule 3
	d, Å			
Re–O	1.700(2)	1.694(3) 1.704(3)	1.693(4) 1.700(3)	1.688(4) 1.692(3)
Re-S_S	2.2788(5)	2.297(1) 2.285(1)	2.297(1) 2.297(1)	2.295(1) 2.288(1)
Re–S_R	2.2978(5)	2.307(1) 2.322(1)	2.325(1) 2.303(1)	2.329(1) 2.316(1)
Re–N (trans to O)	2.239(2)	2.253(4) 2.238(4)	2.255(4) 2.253(4)	1.692(3) 2.264(4)
Re–N (trans to SR)	2.211(2)	2.191(4) 2.173(4)	2.169(4) 2.169(4)	2.160(4) 2.191(4)
Re–N (trans to SS)	2.157(2)	2.142(4) 2.155(4)	2.156(4) 2.153(4)	2.136(4) 2.150(4)
S–S	2.1023(1)	2.109(2)	2.112(2)	2.101(2)
Angle	ω, deg			
ReSC	124.00(8)	123.6(2) 120.64(2)	125.7(2) 121.4(2)	120.3(2) 119.0(2)
ReSS	109.89(3)	109.03(6) 112.36(6)	114.47(6) 116.19(6)	110.78(6) 111.34(6)
ReSSRe	112.98(3)	172.43(4)	128.07(6)	172.47(5)

Complex **I** can also be synthesized by the substitution of the chloride ligand in $TpReOCl(S^tBu)$ by the disulfide anion. The highest yield was only 16% in the reaction with a Na_2S_2 excess in dimethoxyethane where a mixture of unidentified products insoluble in toluene or CH_2Cl_2 was also formed. The crystallization of these products from dimethylformamide and diethyl ether with an additive of tetraphenylphosphonium chloride makes it possible to isolate a minor amount of red-orange crystals with the cell parameters close to those of $[Ph_4P][ReS_4]$ [24]. The reaction with more soluble Li_2S_2 in tetrahydrofuran leads to the fast disappearance of the initial complex, but complex **I** is formed only in trace amounts according to the TLC data.

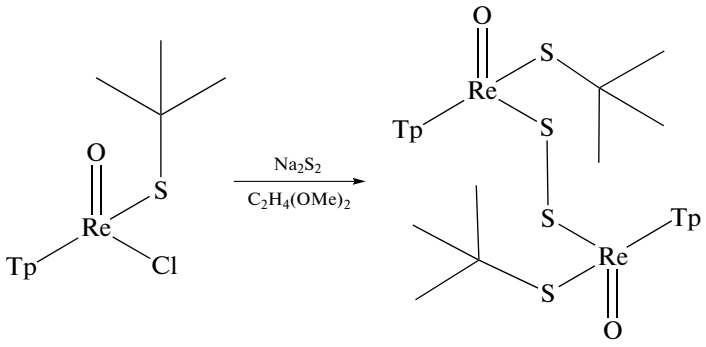

The IR spectrum of compound **I** differs slightly from the spectrum of the initial $TpReO(S^tBu)_2$ complex: a weak absorption peak appears at 917 cm^{-1} and the relative intensity of the series of CH bending vibration bands (especially pronounced for frequencies of 1473, 1406, 1159, 1047, 936, 766, and 756 cm^{-1}) decreases, most likely, due to a change in the ratio of the amounts of pyrazolate and *tert*-butyl groups.

The ^1H NMR spectrum of complex **I** contains nine signals of the pyrazole protons corresponding to the tris(pyrazolyl)borate ligand coordinated to the rhenium atom together with three different substituents

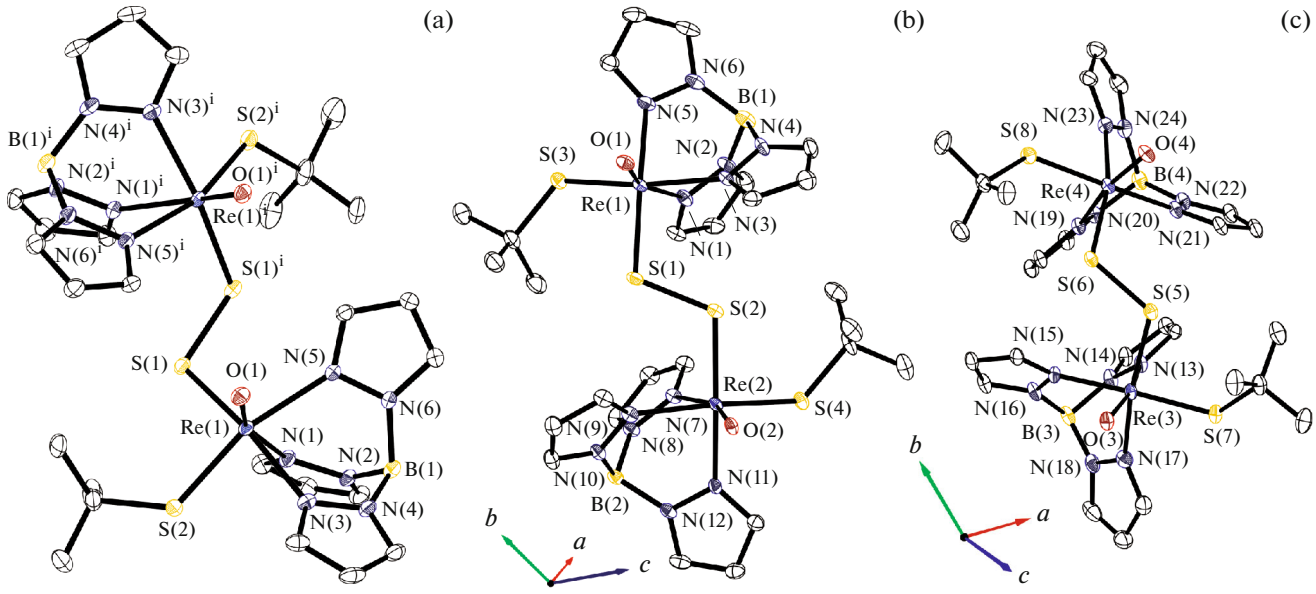

Fig. 1. Molecular structures of compounds (a) **Ia**, (b) **Ib** molecule 1, and (c) **Ib** molecule 2 (independent molecules for **Ib** are shown in particular projections).

and the singlet signal of the *tert*-butyl group. Unlike the initial compound, no properties of dynamic processes are observed in the ^{1}H NMR spectrum of complex **I** at room temperature.

The crystallization of complex **I** by the diffusion of pentane vapors into its solution in CH_2Cl_2 gives crystals of two types **Ia** and **Ib**, whose structures were determined by XRD (Fig. 1). Both crystals contain a racemic mixture of chiral molecules of complex **I** (two rhenium atoms in the dimeric molecule are of the same chirality). The crystal of compound **Ia** (monoclinic crystal system) contains both the molecule of the complex lying on the second-order screw axis and the disordered CH_2Cl_2 molecule. The crystal of triclinic crystal system contains three independent molecules of compound **I**, one molecule of CH_2Cl_2, and a cavity the contents of which is refined as a mixture of CH_2Cl_2 and pentane in a ratio of ~2 : 1.

Different conformations of complex **I** found in the crystals of compounds **Ia** and **Ib** are shown in Fig. 1 (two of three molecules in the packing of **Ib** have nearly identical geometries), and the main geometric parameters are presented in Table 2. Interestingly, all independent molecules of the structures of compounds **Ia** and **Ib** exhibit the same conformation of the ReS_2 fragment in which both substituents at the sulfur atoms do not almost shift from the ReS_2 plane. The single significant distinction in geometries of the observed conformers is a change in the ReSSRe dihedral angles. Conformer **Ib** contains two molecules with the nearly planar ReSSRe fragment and one molecule with an ReSSRe dihedral angle of 128.07(6)°. A higher deviation from the planar structure is observed in compound **Ia** (ReSSRe 112.98(3)°).

The change in the ReSSRe dihedral angle only insignificantly affects other geometric parameters, and the further consideration of the structure of **Ia** as an example can be attributed to other conformers as well.

The ReN distances in complex **I** are noticeably nonequivalent (2.239(2), 2.211(2), 2.157(2) Å for the bonds in the *trans*-position to O, S-*tert*-Bu, and μ-S_2, respectively), most likely, due to a difference in the trans effects of three different substituents. The short Re–O distance (1.700(2) Å) is insignificantly elongated compared to 1.682(4) Å in the dithiolate complex $TpReO(S^tBu)_2$. The Re–S bond lengths with both the thiolate (2.2978(5) Å) and disulfide (2.2788(5) Å) sulfur atoms are appreciably shortened compared to the sum of covalent radii of Re and S (2.56 Å) [25], and the shortening is even slightly noticeable for the disulfide ligand. Interestingly, no considerable increase in the CSRe angle (124.00(8)°) over the ideal tetrahedral angle is observed for the disulfide ligand ReSS (109.89(3)°).

The calculation search for conformers by the semiempirical XTB-GFN2 method followed by the geometry optimization and DFT calculation of the energy for complex **I** gives the lowest energy for the conformer in the crystal of **Ia** observed by XRD. A similar search for the conformers and calculation of the energy for the meso form (two rhenium atoms are of different chirality) shows that its formation is thermodynamically less favorable by 3.5 kcal/mol.

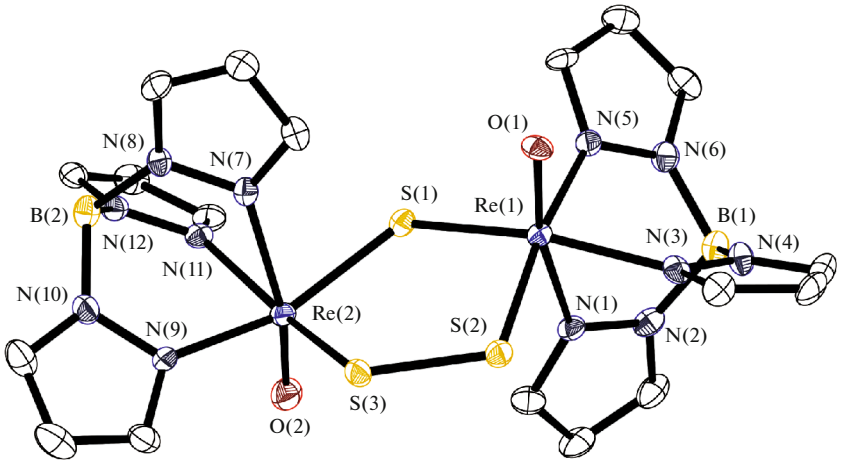

Fig. 2. Molecular structure of compound **II** (solvate molecule of dichloromethane is omitted). Selected bond lengths: Re(1)–O(1) 1.702(4), Re(2)–O(2) 1.687(4), Re(1)–S(1) 2.320(1), Re(2)–S(1) 2.335(1), Re(1)–S(2) 2.237(2), Re(2)–S(3) 2.251(2), Re(1)–N(1) 2.251(5), Re(1)–N(3) 2.138(5), Re(1)–N(5) 2.165(5), Re(2)–N(7) 2.270(5), Re(2)–N(9) 2.106(5), Re(2)–N(11) 2.176(5), and S(2)–S(3) 2.122(2) Å and bond angles: Re(1)S(1)Re(2) 119.84(6)°, S(3)S(2)Re(1) 113.75(7)°, and S(2)S(3)Re(2) 113.74(8)°.

The structure of complex **II** was also determined by XRD (Fig. 2). Two TpReO fragments are linked by the sulfide and disulfide bridging ligands, and the Re_2S_3 cycle turns out to be nearly planar (deviation of the sulfur atoms of the disulfide bridge from the plane is 0.18 Å). The Re–S bonds with the disulfide ligand (2.237(2), 2.251(2) Å) are shortened even more strongly than those in the thiolate disulfide complex, whereas the bonds with the sulfide bridge are shortened to a lower extent (2.320(1), 2.3351(1) Å), because, most likely, only one lone pair of sulfur participates in the additional π bonding with the rhenium atoms. A similar distribution of the metal–sulfur distances was observed in the Re_2S_3 cycles of the chain tetranuclear Re(V) complex $[NEt_4]_2[((Me_3Si)_2C_2S_2)_2$-$Re_4(S)_4(\mu\text{-}S)_4(\mu\text{-}S_2)_2]$ [26]. For the molybdenum(V) complex $[Tp^{iPr}MoO]_2(\mu\text{-}S_2)(\mu\text{-}S)$ similar in structure to complex **II** [27], a higher electron deficiency results in an appreciable increase in the MoSMo angle (136.5°) and the bonds with the sulfide bridge (2.28 Å) turn out to be shorter than those with the disulfide bridge (2.33 Å).

Thus, it was shown that the rhenium(V) tris(pyrazolyl)borate disulfide complex with thiolate ligands can be synthesized by both the dealkylation of the *tert*-butylthiolate group and substitution of the chloride ligand by the disulfide anion.

ACKNOWLEDGMENTS

The studies were carried out using the equipment of the of the Center for Collective Use of Physical Methods of Investigation at the Kurnakov Institute of General and Inorganic Chemistry (Russian Academy of Sciences).

FUNDING

This work was supported by the Russian Science Foundation, project no. 18-73-10206.

CONFLICT OF INTEREST

The authors of this work declare that they have no conflicts of interest.

REFERENCES

1. Trofimenko, S., *Chem. Rev.*, 1993, vol. 93, p. 943.
2. Lail, M., Pittard, K.A., and Gunnoe, T.B., *Adv. Organomet. Chem.*, 2008, vol. 56, p. 95.
3. Tisato, F., Bolzati, C., Duatti, A., et al., *Inorg. Chem.*, 2042, vol. 32, no. 10.
4. Doonan, C.J., Nielsen, D.J., Smith, P.D., et al., *J. Am. Chem. Soc.*, 2006, vol. 128, p. 305.
5. McWhinnie, S.L.W., Jones, C.J., McCleverty, J.A., et al., *Polyhedron*, 1993, vol. 12, p. 3743.
6. Wei, L.-P., Ren, Z.-G., Zhu, L.-W., et al., *Inorg. Chem.*, 2011, vol. 50, p. 4493.
7. Arikawa, Y., Otsubo, Y., Nakayama, T., et al., *Inorg. Chim. Acta*, 2019, vol. 490, p. 45.
8. Skabitskii, I.V., Sakharov, S.G., Pasynskii, A.A., et al., *Russ. J. Coord. Chem.*, 2019, vol. 45, p. 539.
9. *SADABS (version 2008/1)*, Madison: Bruker AXS Inc., 2008.
10. Sheldrick, G.M., *TWINABS (version 2012/1)*, Madison: Bruker AXS Inc., 2012.
11. Sheldrick, G.M., *Acta Crystallogr., Sect. A: Found. Crystallogr.*, 2008, p. 112.
12. Dolomanov, O.V., Bourhis, L.J., Gildea, R.J., et al., *J. Appl. Crystallogr.*, 2009, vol. 42, p. 339.

13. Neese, F., *The ORCA Program System. Wiley Interdisciplinary Reviews—Computational Molecular Science*, 2012, vol. 2, p. 73.
14. Perdew, J.P., Burke, K., and Ernzerhof, M., *Phys. Rev. Lett.*, 1996, vol. 77, p. 3865.
15. Perdew, J.P., Burke, K., and Ernzerhof, M., *Phys. Rev. Lett.*, 1997, vol. 78, p. 1396.
16. Weigend, F. and Ahlrichs, R., *Phys. Chem. Chem. Phys.*, 2005, vol. 7, p. 3297.
17. Grimme, S., Ehrlich, S., and Goerigk, L., *J. Comput. Chem.*, 2011, vol. 32, p. 1456.
18. Grimme, S., Antony, J., Ehrlich, S., et al., *J. Chem. Phys.*, 2010, vol. 132, p. 154104.
19. Adamo, C. and Barone, V., *J. Chem. Phys.*, 1999, vol. 110, p. 6158.
20. van Lenthe, E., Baerend, E.J., and Snijders, J.B., *J. Chem. Phys.*, 1993, vol. 99, p. 4597.
21. van Wüllen, C., *J. Chem. Phys.*, 1998, vol. 109, p. 392.
22. Rolfes, J.D., Neese, F., and Pantazis, D.A., *J. Comput. Chem.*, 2020, vol. 41, p. 1842.
23. Pantazis, D.A., Chen, X.Y., Landis, C.R., et al., *J. Chem. Theory Comput.*, 2008, vol. 4, p. 908.
24. Diemann, E. and Muller, A., *Z. Naturforsch., A: Phys. Sci.*, 1976, vol. 31, p. 1287.
25. Cordero, B., Gomez, V., and Platero-Prats, A.E., *Dalton Trans.*, 2008, vol. 21, p. 2832.
26. Goodman, J.T. and Rauchfuss, T.B., *Inorg. Chem.*, 1998, vol. 37, p. 5040.
27. Gourlay, C., Taylor, M.K., Smith, P.D., et al., *Inorg. Chim. Acta*, 2010, vol. 363, p. 1126.

Translated by E. Yablonskaya